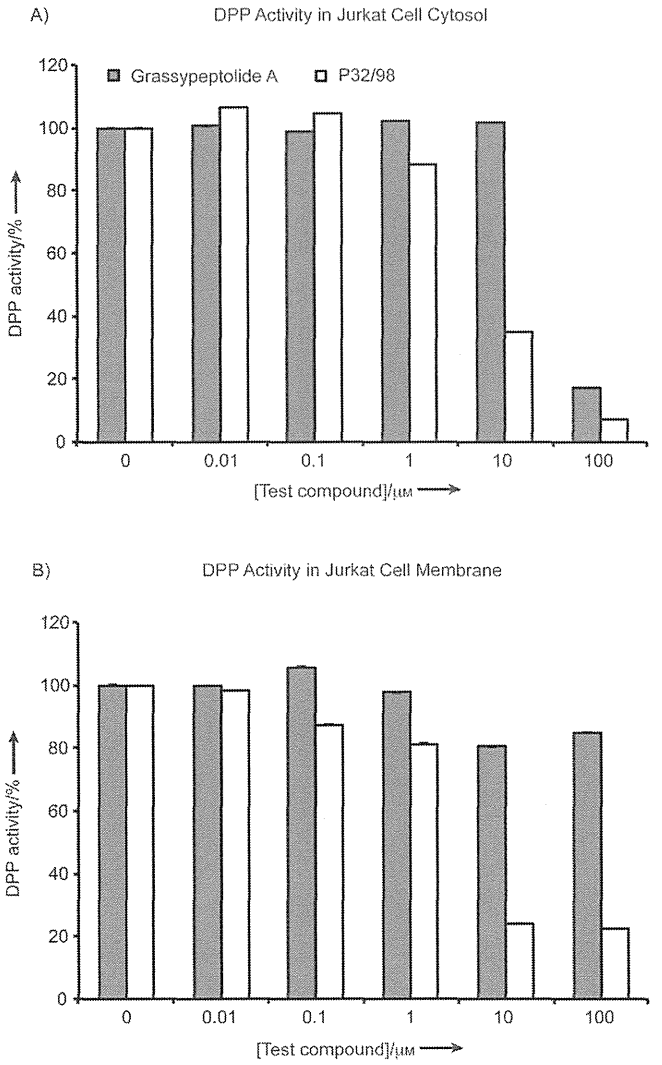

Figure 4. Effect of grassypeptolide A (**1**) on DPP activity in A) Jurkat cell cytosol, and B) Jurkat cell membrane fractions.

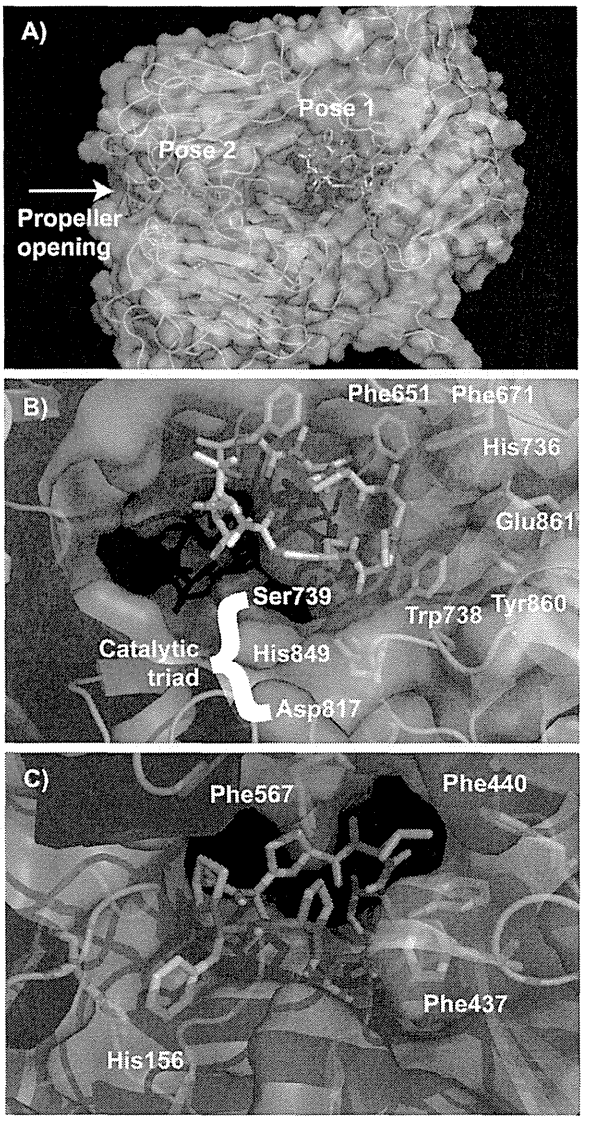

Figure 5. Two docked poses of grassypeptolide A (**1**) generated by in silico molecular docking into a homology model of DPP8. A) Overview of the two identified binding sites. B) Close-up of pose 1 (close to active site), showing the catalytic triad and aromatic residues close to the *N*-Me-Phe unit of **1**. C) Close-up of pose 2 (inside surface of propeller opening), showing aromatic residues close to the phenyl rings or other π bonds of **1**.

residues (Phe651, Phe671, His736, Trp738 and Tyr860, also known as the T-stacking conserved aromatic motif,[30] see Figure 5). Interestingly, DPP4 possesses an extra aromatic residue in this pocket—Tyr752 (Glu861 in the DPP8 homology model, see Figure S1 in the Supporting Information). If pose 1 is placed in an aligned X-ray structure of DPP4 (PDB ID: 2BGR),[32] it can be seen that a steric clash would occur between the *N*-Me-Phe and Tyr752. Compound **1** does dock into DPP4 at this site, but the *N*-Me-Phe is not bound so deeply in the aromatic pocket (see Figure S1). Potentially, deeper binding of the *N*-Me-Phe side chain in the pocket could perturb the relative positions of the β-sheet and α-helix that are attached to the active-site residues Ser739 and His849, respectively.

Likewise, at the propeller opening site (pose 2), there are several aromatic residues that could engage in π–π interactions to **1** (His156, Phe437, Phe440, Phe567, see Figure 5). In DPP4 these are replaced by Ser106, Glu361, His363 and Lys463, respectively, and so **1** docks into DPP4 at this site with a different orientation, in which there is a likely edge-to-face π–π interaction with Trp215 (see Figure S1). Binding at this site would effectively block the propeller opening in both DPP4 and DPP8, and therefore might disproportionately affect cleavage of substrates that use this entrance. Because the substrate used in our enzymatic inhibition experiments (H-GP-AMC) is fairly small, inhibition by blocking the propeller opening might not have been detected. In light of the docking results, the mode of inhibition might simply be steric hindrance of the substrate around the active site, along with prevention of its entrance through the propeller opening. Both of these might be more effective inhibition strategies against larger substrates, and this could potentially explain the fairly high IC_{50} values when measured with a small substrate (H-GP-AMC), relative to the effect on T-cells. Some candidate substrates for

DPP8 have been identified through proteomics,[25] and all of them are proteins containing more than 200 amino acids. These larger substrates might require the propeller opening, or they might be less able than a smaller substrate to displace **1** from the active site.

We have shown that the grassypeptolides inhibit DPP8, and molecular docking suggests that **1** might bind to the inner cavity of the enzyme at two distinct sites. The compound thus might prove to be a valuable tool for studying the relative importance of the propeller opening for different substrates when they are identified.

Experimental Section

Isolation of grassypeptolides: The grassypeptolides were isolated from samples of *L. confervoides* as previously described.[11] After natural sources of grassypeptolide A were exhausted, material obtained through total synthesis[12] was used.

Protease inhibition screen: The initial protease screen was carried out as previously described,[7] by Reaction Biology Corp. (Malvern, PA, with 20 μM **1**). Follow-up experiments to determine the IC_{50} values of **1**–**3** used the same conditions as for the screen but with a range of concentrations for the test compounds, each in duplicate.

T-cell IL-2 and proliferation assay: Human CD3+ T-cells were purified from peripheral blood mononuclear cells from a healthy adult volunteer, with use of a MACS Pan T-cell Isolation Kit (Miltenyi Biotech). A 96-well plate was coated with murine anti-CD3 (OKT3, 0.5 μg mL^{-1}) and anti-CD28 (4B10, 5 μg mL^{-1}) as previously described.[33] T-cells were added to the precoated plate (1×10^5 cells/well), and incubated in serum-free AIM-V medium in the presence of different concentrations of grassypeptolide A (**1**, added as a solution in DMSO) for 48 h. Concentrations of IL-2 in the supernatants were then quantified by sandwich ELISA. To quantify proliferation, cells were grown under the same conditions for 48 h, after which time MTT dye was added to wells in order to measure relative cell number.

Jurkat IL-2 and viability assay: Jurkat cells were grown in 96-well plates (100000 cells/well), in RPMI-1640 medium in the presence of PMA (80 nM, Sigma–Aldrich, added as a solution in DMSO), PHA (10 μg mL^{-1}, Sigma–Aldrich, added as a solution in PBS), and varying concentrations of **2** or **3** (added as 100-fold freshly prepared stock solutions in EtOH), by the procedure of Fischer et al.[28] The DMSO content of the culture wells was kept below 0.25% because it was found to be toxic to Jurkat cells at higher levels. After 24 h incubation at 37 °C in a humidified atmosphere containing CO_2 (5%), the IL-2 content of the supernatants was quantified with the aid of a hIL-2 alphaLISA kit and an EnVision detector (PerkinElmer). To quantify viability, cells were grown under the same conditions and then developed with MTT dye by the manufacturer's protocol (Promega).

Jurkat cell endogenous DPP activity assay: Jurkat cells were grown and subjected to subcellular fractionation as described by Rockstroh et al.[34] Various concentrations of compound or solvent control, subcellular fractions and substrate were preincubated for 10 min at 37 °C, after which the absorbance at 405 nm was monitored for 5 min with a microplate reader.[35] The slope was used to quantify enzyme activity. The amount of protein in the cytosolic/membrane fraction used for each reaction was 500 μg, obtained from 5×10^6 cells. DPP8/9 and DPP4 activity were determined separately in cytosolic and membrane fractions with the substrate Gly-Pro-pNA [0.5 mM in Tris buffer (pH 8.3, 0.05 M) containing EDTA (10 mM) and aprotinin (14 μg mL^{-1})]. Both Gly-Pro-pNA and P32/98 (positive control inhibitor) were obtained from Enzo (Farmingdale, NY).

Molecular docking: A previously determined crystal structure of compound **1**[10] was docked into DPP4 and DPP8 by use of Autodock Vina 1.1.1,[36] with an exhaustiveness value of 100 and with a search box encompassing the entire interior of the appropriate protein. A previously published homology model of DPP8 was used[30] because no crystal structure is available. The crystal structure 2BGR was used for docking to DPP4[32] because this structure was the basis of the DPP8 homology model. The two proteins were aligned to each other in PyMOL (Schrödinger, LLC) prior to docking in order to aid comparison between the docking poses of each. Each docking run produced 100 binding modes, which were examined in ascending order of calculated binding energy. The binding poses shown in Figure 5 are the lowest-binding-energy structures of the two binding sites found in the total set of binding modes.

Acknowledgements

This research was supported in part by the National Institutes of Health, NIGMS grant P41GM086210 and NCI grant R01CA172310. We wish to thank Christian Rummey for kindly providing the homology model of DPP8. We would also like to thank Nam Dang for helpful discussions. This is contribution 940 from the Smithsonian Marine Station at Fort Pierce.

Keywords: dipeptidyl peptidases · grassypeptolides · immunochemistry · natural products · protease inhibition

[1] C. López-Otín, J. S. Bond, *J. Biol. Chem.* **2008**, *283*, 30433–30437.
[2] B. Turk, *Nat. Rev. Drug Discovery* **2006**, *5*, 785–799.
[3] D. J. Newman, G. M. Cragg, *J. Nat. Prod.* **2012**, *75*, 311–335.
[4] L. T. Tan, *Phytochemistry* **2007**, *68*, 954–979.
[5] J. C. Kwan, K. Taori, V. J. Paul, H. Luesch, *Mar. Drugs* **2009**, *7*, 528–538.
[6] L. A. Salvador, K. Taori, J. S. Biggs, J. Jakoncic, D. A. Ostrov, V. J. Paul, H. Luesch, *J. Med. Chem.* **2013**, *56*, 1276–1290.
[7] J. C. Kwan, E. A. Eksioglu, C. Liu, V. J. Paul, H. Luesch, *J. Med. Chem.* **2009**, *52*, 5732–5747.
[8] P. G. Williams, W. Y. Yoshida, R. E. Moore, V. J. Paul, *J. Nat. Prod.* **2003**, *66*, 1006–1009.
[9] Y. Liu, W. Zhang, L. Li, L. A. Salvador, T. Chen, W. Chen, K. M. Felsenstein, T. B. Ladd, A. R. Price, T. E. Golde, J. He, Y. Xu, Y. Li, H. Luesch, *J. Med. Chem.* **2012**, *55*, 10749–10765.
[10] J. C. Kwan, J. R. Rocca, K. A. Abboud, V. J. Paul, H. Luesch, *Org. Lett.* **2008**, *10*, 789–792.
[11] J. C. Kwan, R. Ratnayake, K. A. Abboud, V. J. Paul, H. Luesch, *J. Org. Chem.* **2010**, *75*, 8012–8023.
[12] H. Liu, Y. Liu, Z. Wang, X. Xing, A. R. Maguire, H. Luesch, H. Zhang, Z. Xu, T. Ye, *Chem. Eur. J.* **2013**, *19*, 6774–6784.
[13] C. C. Thornburg, M. Thimmaiah, L. A. Shaala, A. M. Hau, J. M. Malmo, J. E. Ishmael, D. T. A. Youssef, K. L. McPhail, *J. Nat. Prod.* **2011**, *74*, 1677–1685.
[14] W. L. Popplewell, R. Ratnayake, J. A. Wilson, J. A. Beutler, N. H. Colburn, C. J. Henrich, J. B. McMahon, T. C. McKee, *J. Nat. Prod.* **2011**, *74*, 1686–1691.
[15] A. Bertram, G. Pattenden, *Nat. Prod. Rep.* **2007**, *24*, 18–30.
[16] W. E. Houssen, M. Jaspars, *ChemBioChem* **2010**, *11*, 1803–1815.
[17] P. Van der Veken, A. Soroka, I. Brandt, Y.-S. Chen, M.-B. Maes, A.-M. Lambeir, X. Chen, A. Haemers, S. Scharpé, K. Augustyns, I. De Meester, *J. Med. Chem.* **2007**, *50*, 5568–5570.

[18] S. Van Goethem, P. Van der Veken, V. Dubois, A. Soroka, A.-M. Lambeir, X. Chen, A. Haemers, S. Scharpé, I. De Meester, K. Augustyns, *Bioorg. Med. Chem. Lett.* **2008**, *18*, 4159–4162.
[19] S. Van Goethem, V. Matheeussen, J. Joossens, A.-M. Lambeir, X. Chen, I. De Meester, A. Haemers, K. Augustyns, P. Van der Veken, *J. Med. Chem.* **2011**, *54*, 5737–5746.
[20] C. F. Deacon, *Diabetes Obes. Metab.* **2011**, *13*, 7–18.
[21] D. M. T. Yu, K. Ajami, M. G. Gall, J. Park, C. S. Lee, K. A. Evans, E. A. McLaughlin, M. R. Pitman, C. A. Abbott, G. W. McCaughan, M. D. Gorrell, *J. Histochem. Cytochem.* **2009**, *57*, 1025–1040.
[22] J. Schade, M. Stephan, A. Schmiedl, L. Wagner, A. J. Niestroj, H.-U. Demuth, N. Frerker, C. Klemann, K. A. Raber, R. Pabst, S. von Hörsten, *J. Histochem. Cytochem.* **2008**, *56*, 147–155.
[23] R. Geiss-Friedlander, N. Parmentier, U. Möller, H. Urlaub, B. J. Van den Eynde, F. Melchior, *J. Biol. Chem.* **2009**, *284*, 27211–27219.
[24] T.-W. Yao, W.-S. Kim, D. M. T. Yu, G. Sharbeen, G. W. McCaughan, K.-Y. Choi, P. Xia, M. D. Gorrell, *Mol. Cancer Res.* **2011**, *9*, 948–959.
[25] C. H. Wilson, D. Indarto, A. Doucet, L. D. Pogson, M. R. Pitman, K. McNicholas, R. I. Menz, C. M. Overall, C. A. Abbott, *J. Biol. Chem.* **2013**, *288*, 13936–13949.
[26] G. R. Lankas, B. Leiting, R. S. Roy, G. J. Eiermann, M. G. Beconi, T. Biftu, C.-C. Chan, S. Edmondson, W. P. Feeney, H. He, D. E. Ippolito, D. Kim, K. A. Lyons, H. O. Ok, R. A. Patel, A. N. Petrov, K. A. Pryor, X. Qian, L. Reigle, A. Woods, et al., *Diabetes* **2005**, *54*, 2988–2994.
[27] U. Schneider, H.-U. Schwenk, G. Bornkamm, *Int. J. Cancer* **1977**, *19*, 621–626.
[28] B. S. Fischer, D. Qin, K. Kim, T. V. McDonald, *J. Pharmacol. Exp. Ther.* **2001**, *299*, 238–246.
[29] H.-K. Tang, K.-C. Chen, G.-G. Liou, S.-C. Cheng, C.-H. Chien, H.-Y. Tang, L.-H. Huang, H.-P. Chang, C.-Y. Chou, X. Chen, *FEBS Lett.* **2011**, *585*, 3409–3414.
[30] C. Rummey, G. Metz, *Proteins Struct. Funct. Bioinf.* **2007**, *66*, 160–171.
[31] S. Nordhoff, S. Cerezo-Gálvez, A. Feurer, O. Hill, V. G. Matassa, G. Metz, C. Rummey, M. Thiemann, P. J. Edwards, *Bioorg. Med. Chem. Lett.* **2006**, *16*, 1744–1748.
[32] W. A. Weihofen, J. Liu, W. Reutter, W. Saenger, H. Fan, *J. Biol. Chem.* **2005**, *280*, 14911–14917.
[33] R.-P. Dong, Y. Umezawa, H. Ikushima, Y. Munakata, S. F. Schlossman, C. Morimoto, *J. Clin. Immunol.* **1997**, *17*, 247–252.
[34] M. Rockstroh, S. A. Müller, C. Jende, A. Kerzhner, M. von Bergen, J. M. Tomm, *J. Integr. OMICS* **2011**, *1*, 135–143.
[35] M.-B. Maes, V. Dubois, I. Brandt, A.-M. Lambeir, P. Van der Veken, K. Augustyns, J. D. Cheng, X. Chen, S. Scharpé, I. De Meester, *J. Leukocyte Biol.* **2007**, *81*, 1252–1257.
[36] O. Trott, A. J. Olson, *J. Comput. Chem.* **2010**, *31*, 455–461.

Received: December 4, 2013
Published online on March 3, 2014

Clinical Investigations

Respiration

Respiration 2014;88:277–284
DOI: 10.1159/000364948

Received: February 5, 2014
Accepted after revision: May 29, 2014
Published online: August 28, 2014

Asbestos-Related Diffuse Pleural Thickening

Nobukazu Fujimoto[a] Katsuya Kato[c] Ikuji Usami[d] Fumikazu Sakai[e]
Takeshi Tokuyama[f] Seiji Hayashi[g] Kenji Miyamoto[h] Takumi Kishimoto[b]

Departments of [a]Medical Oncology and [b]Internal Medicine, Okayama Rosai Hospital, and [c]Department of Radiology, Okayama University Hospital, Okayama, [d]Department of Internal Medicine, Asahi Rosai Hospital, Owariasahi, [e]Department of Radiology, Saitama Medical University International Medical Center, Hidaka, [f]Department of Internal Medicine, Saiseikai-Chuwa Hospital, Sakurai, [g]Department of Respiratory Medicine, Kinki-Chuo Chest Medical Center, Sakai, and [h]Faculty of Health Sciences, Hokkaido University, Sapporo, Japan

Key Words

Asbestos · Pleural thickening · Medical Research Council dyspnea scale · Respiratory function test · Pleural plaques · Blunted costophrenic angle · Imaging

Abstract

Background: The clinical features of asbestos-related diffuse pleural thickening (DPT) remain unclear. ***Objectives:*** To clarify the association between radiological findings of DPT and respiratory function. ***Methods:*** Medical data from patients with asbestos-related DPT were collected, including their history of occupational or neighborhood asbestos exposure, initial symptoms, modified Medical Research Council dyspnea grade, smoking history, radiological findings, and respiratory function test results. ***Results:*** There were 106 DPT patients between 2005 and 2010 [i.e. 103 men (97.2%) and 3 women (2.8%)]. The median age at diagnosis was 69 years (range 46–88). Patient occupations related to asbestos exposure included: asbestos product manufacturing (n = 17); the shipbuilding industry (n = 14); the construction industry (n = 13); heat insulation work (n = 12); plumbing, asbestos spraying, and electrical work (n = 7 each), and transportation and demolition work (n = 4 each). The median duration of asbestos exposure was 25 years (range 2–54), and the median latency period before the onset of DPT was 46 years (range 25–66). Involvement of the costophrenic angle (CPA) was also negatively correlated with the percent vital capacity (%VC; $r = -0.448$, $p < 0.01$). Pleural thickness and the craniocaudal and horizontal extension of pleural thickening, as determined by chest computed tomography (CT), were also negatively correlated with %VC ($r = -0.226$, $p < 0.05$; $r = -0.409$, $p < 0.01$, and $r = -0.408$, $p < 0.01$, respectively). ***Conclusions:*** DPT develops after a long latency period following occupational asbestos exposure and causes marked respiratory dysfunction. The extension of DPT should be evaluated by chest CT, and chest X-ray would be important for the evaluation of the involvement of the CPA.

Introduction

Asbestos-related pleural diseases include malignant pleural mesothelioma, benign asbestos pleural effusion (BAPE), and diffuse pleural thickening (DPT) [1]. DPT often develops after the onset of BAPE [2, 3]; however,

KARGER

E-Mail karger@karger.com
www.karger.com/res

0025–7931/14/0884–0277$39.50/0

Nobukazu Fujimoto, MD, PhD
Department of Medical Oncology, Okayama Rosai Hospital
1-10-25 Chikkomidorimachi
Okayama 7028055 (Japan)
E-Mail nobufujimot@gmail.com

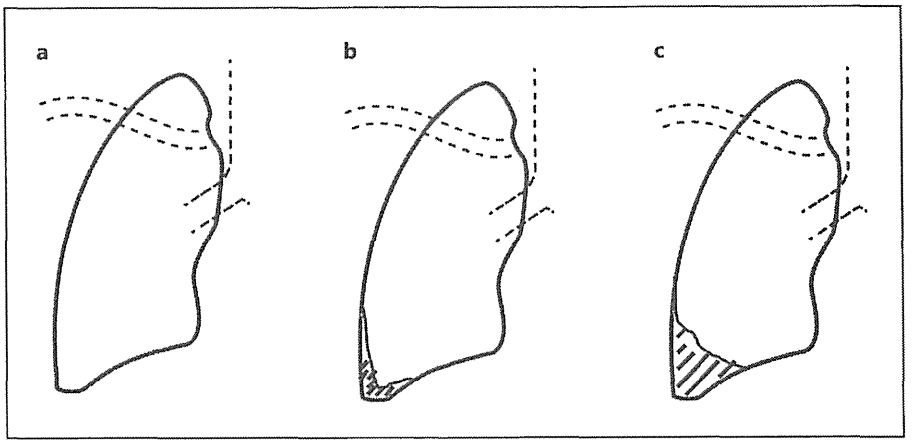

Fig. 1. Examples of the involvement of the CPA on chest X-ray. **a** No involvement (0). **b** CPA ≤90° (1). **c** CPA >90° (2).

some patients develop DPT in the absence of BAPE. Asbestos-related DPT is considered to be a consequence of asbestos-induced inflammation of the visceral pleura, which leads to adhesion to the parietal pleura [4]; however, the actual pathogenesis is unknown.

DPT is not precisely defined in radiological terms [5]. McLoud et al. [6] described DPT on chest X-ray as a smooth, noninterrupted pleural density extending over at least one fourth of the chest wall with or without involvement of the costophrenic angle (CPA). However, these criteria are somewhat ambiguous. In addition, radiological differentiation between DPT and pleural plaques is often difficult. The revised 2000 International Labour Organization Classification of Radiographs of Pneumoconioses provides a criterion for the differentiation between pleural plaques and DPT, in which involvement of the CPA should be demonstrated for DPT [7]. However, the validity of this criterion is still controversial. Some studies have examined the characteristics and natural history of DPT [2, 5, 6, 8–10]. One of the main limitations of these earlier studies is that the definitions used for DPT varied; a significant proportion of the studies included patients with pleural plaques, BAPE, and malignant pleural mesothelioma, mainly due to the difficulty of making differential diagnoses based on chest X-rays without computed tomography (CT) images.

In this study, we investigated the clinical features of DPT. Our main purpose was to clarify the association between DPT and asbestos exposure. In addition, we focused on the association between radiological findings and respiratory function. For this purpose, we analyzed the extension of DPT on chest CT images in detail using our own scoring methods, and we examined its association with impaired respiratory function.

Methods

Patients

All of the subjects diagnosed with DPT at each of the researchers' institution were extracted. Medical data from those patients were collected and analyzed retrospectively. Inclusion criteria were a history of occupational or neighborhood asbestos exposure and pleural thickening >5 mm on chest X-ray extending for more than half of the lateral thoracic wall (LTW) in patients with unilateral DPT or for more than a quarter of the LTW in patients with bilateral DPT. The medical information we collected included the initial symptoms, the modified Medical Research Council (mMRC) dyspnea grade, the smoking history, radiological findings, and respiratory function test results. Information about the history of asbestos exposure and the mMRC dyspnea grade was also collected at the diagnosis. The respiratory function test was based on the official statement of the American Thoracic Society [11]. To examine the association between radiological findings and respiratory function, chest images and the results of respiratory function tests undergone within a year were extracted. This study was approved by the Japan Labour Health and Welfare Organization and the institutional review boards of each institution.

Radiological Analyses

The chest X-ray findings we examined included the craniocaudal extension of pleural thickening and the involvement of the CPA. Craniocaudal extension was classified and scored as 0 (none), 1 (total length up to one quarter of the projection of the LTW), 2 (total length exceeding one quarter and up to one half of the projection of the LTW), or 3 (total length exceeding one half of the projection of the LTW) in accordance with the International Labour Organization classification [7]. The involvement of the CPA was also determined and classified into 3 categories: 0 (no involvement), 1 (CPA ≤90°), or 2 (CPA >90°) (fig. 1).

The thickness of the pleura and the craniocaudal extension were also determined by chest CT. The thickness of the pleura was determined and scored as 0 (none), 1 (<3 mm), 2 (3–5 mm), 3 (5–10 mm), or 4 (>10 mm). To assess the craniocaudal extension of pleural thickening, the thorax was divided into 5 zones according to the upper border of the aortic arch, the tracheal bifurcation, the inflow portion of the left inferior pulmonary vein to the heart,

and the upper border of the diaphragm (fig. 2). The number of involved zones was scored as 0–5. The horizontal extension was determined in the most involved zone and scored as 0 (no involvement), 1 (less than a quarter of the outer perimeter of the thorax), 2 (between a quarter and half of the outer perimeter of the thorax), or 3 (more than half of the outer perimeter of the thorax). The total scores in individual cases were calculated as the sum of both sides of the pleura. Other items that were analyzed by chest CT included pleural plaques, crow's feet signs (defined as fibrous strands with accompanying pleural circumscribed thickening), fibrotic changes, and emphysematous findings.

For all of the radiological analyses, the researchers were divided in 2 groups, both of which comprised at least 1 radiation and 2 respiratory specialists. The radiological findings were analyzed independently by each group. In cases in which the results differed between the 2 groups, 2 radiologists (K.K. and F.S.) and the chairman (T.K.) discussed to reach a final agreement.

Respiratory Function Test

Respiratory function tests were performed in clinical practice. The data included the percent vital capacity (%VC) and the forced expiratory volume percentage in 1 s (FEV_1). The ratio of FEV_1 to forced vital capacity (FVC) was also calculated as FEV_1/FVC. Blood gas data such as PaO_2 and $PaCO_2$ were also extracted. The data closest in time to when the chest CT was performed were used for the analyses.

Statistical Analysis

Pearson's rank correlation coefficient was calculated for the correlation between respiratory function and radiological findings. Cohen's kappa coefficient (κ) was calculated for intergroup agreement [12]. These calculations were performed with SPSS 11.0 software (SPSS, Inc., Chicago, Ill., USA).

Results

Patient Characteristics

We collected and analyzed data from 106 patients diagnosed with DPT between August 1993 and November 2011 (103 men and 3 women). The median age (range) was 70 years (46–88). There were 25 (24.0%) current and 64 (61.6%) former smokers; 15 (14.4%) of the patients had never smoked, while the smoking status of 2 patients was unknown. Forty-five (42.5%) patients had been diagnosed with DPT during a routine medical checkup, and 56 (52.8%) patients had visited a medical institution for subjective complaints, including dyspnea in 45 cases, cough in 38, sputum in 6, chest pain in 5, fever in 3, and weight loss, anorexia, and chest discomfort in 1 patient each. The mMRC dyspnea grade was determined in 96 cases. Fourteen patients (14.6%) were grade 0; 25 (24.0%) were grade 1; 34 (35.4%) were grade 2, and 23 (24.0%) were grade 3 or 4. Fifty-three patients (50.0%) had a medical history of BAPE.

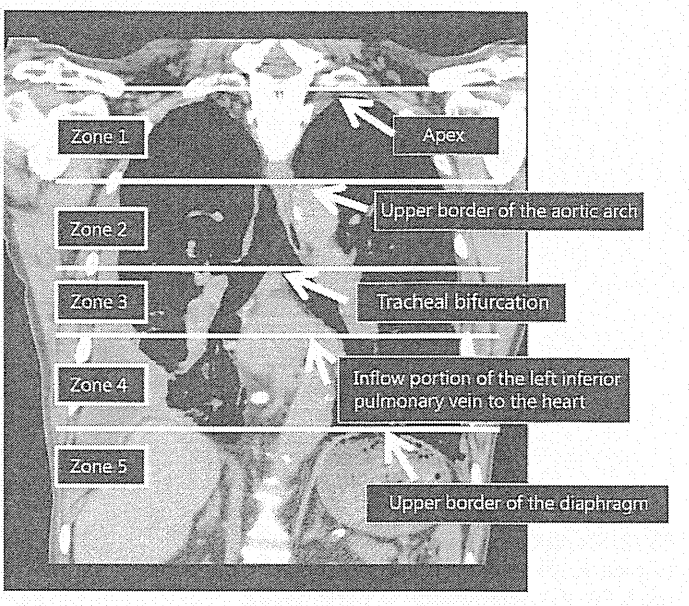

Fig. 2. Examples of a CT image of the thorax divided into 5 zones by the (1) upper border of the aortic arch, (2) tracheal bifurcation, (3) inflow portion of the left inferior pulmonary vein to the heart, and (4) upper border of the diaphragm. These zones were used to assess the craniocaudal extension of pleural thickening.

Table 1. Occupational categories associated with asbestos exposure

Occupation	Cases, n (%)
Asbestos product manufacturing	17 (16)
Shipbuilding	14 (13.2)
Construction	13 (12.3)
Heat insulation work	12 (11.3)
Plumbing	7 (6.6)
Asbestos spraying	7 (6.6)
Electrical work	7 (6.6)
Demolition work	4 (3.8)
Transportation	4 (3.8)
Duct mounting	2 (1.9)
Upholstery work	2 (1.9)
Painting	2 (1.9)
Other	15 (14.2)
Total	106 (100)

Asbestos Exposure History

The occupational categories associated with asbestos exposure are shown in table 1. The median duration of exposure was 25 years (range 2–54), and the median period of latency from the first exposure to the onset of

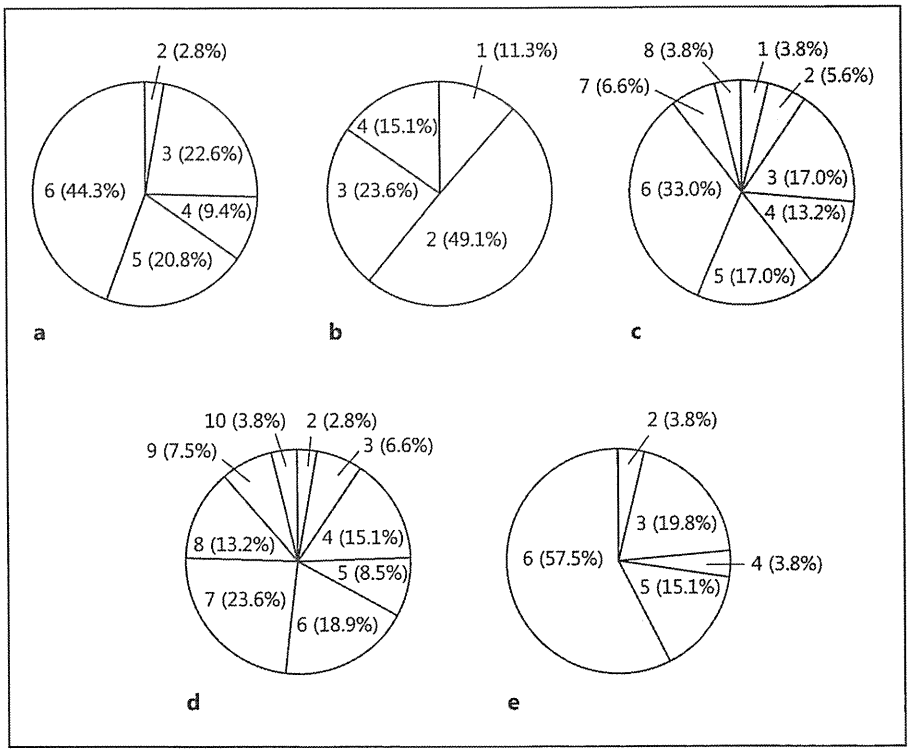

Fig. 3. Scores of the craniocaudal extension of pleural thickening (**a**), involvement of the CPA (**b**) determined on chest X-ray, thickness of the pleura (**c**), craniocaudal extension of pleural thickening (**d**), and horizontal extension (**e**) determined on chest CT. Values are presented as percentages of applicable patients for each score.

Table 2. Existence of radiological findings and Cohen's κ calculated for intergroup agreement

Findings	Existence, n (%)	κ
Pleural plaques	97 (91.5)	0.575
Crow's feet signs	103 (97.2)	0.695
Fibrotic changes	46 (43.4)	0.481
Emphysematous changes	50 (47.2)	0.627

DPT was 47 years (range 25–66). There were no patients in whom neighborhood asbestos exposure was suspected.

Radiological Features

The characteristic radiological findings are summarized in table 2. Asbestosis, defined as a profusion rate >1 based on ILO criteria [7], was present in 7 patients (6.6%).

The craniocaudal extension of pleural thickening, the involvement of the CPA scored on chest X-ray, the thickness of the pleura, the craniocaudal extension of pleural thickening, and the horizontal extension scored on chest CT are shown in figure 3. Cohen's κ for these parameters were 0.206, 0.431, 0.441, 0.843, and 0.565, respectively.

Respiratory Function Test

The median (range) values for %VC and FEV_1/FVC were 54.3% (17.3–99.4) and 79.7% (37.9–100.0), respectively. The median (range) PaO_2 and $PaCO_2$ values were 81.0 mm Hg (52.4–94.8) and 42.7 mm Hg (22.3–73.2), respectively. Constrictive respiratory dysfunction (%VC <80) was found in 96 patients (91.0%), and obstructive respiratory dysfunction (FEV_1/FVC <70) was found in 29 patients (28%). Mixed respiratory dysfunction was found in 25 patients (24.0%).

We next analyzed the correlation between %VC and the extension of DPT as measured on radiological images. The craniocaudal extension of pleural thickening as determined and scored on chest X-ray was negatively correlated with %VC ($r = -0.483$, $p < 0.01$), and involvement of the CPA was also negatively correlated with %VC ($r = -0.448$, $p < 0.01$) (fig. 4). In the 52 cases in which the involvement of the CPA was scored as 2, the %VC tended to be lower in cases with bilateral involvement of the CPA (a score of 1 on each side) than in cases with unilateral involvement (a score of 2 on one side and 0 on the other). However, this difference was not statistically significant ($p = 0.078$). The thickness of the pleura (fig. 5a) and the craniocaudal (fig. 5b) and horizontal (fig. 5c) extension of pleural thickening, as determined

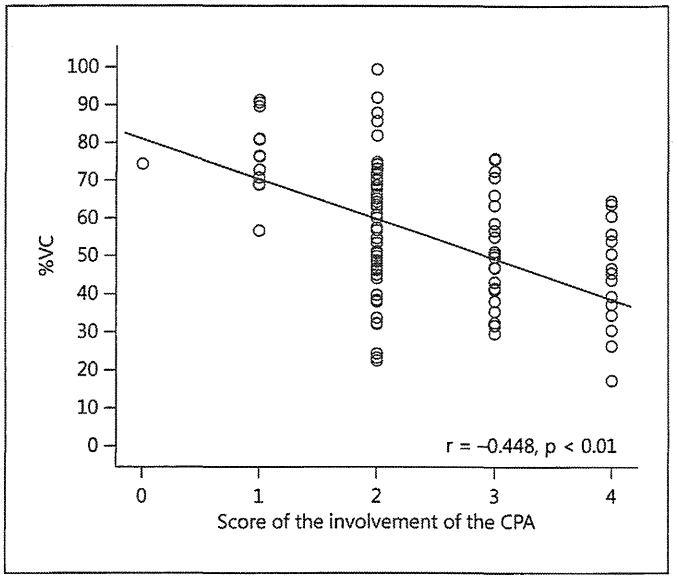

Fig. 4. The correlation between %VC and involvement of the CPA is shown by the correlation coefficient (r) and the regression line.

on chest CT, were also negatively correlated with %VC ($r = -0.226$, $p < 0.05$; $r = -0.409$, $p < 0.01$; and $r = -0.408$, $p < 0.01$, respectively).

Discussion

In the current study, we retrospectively analyzed 106 patients with DPT. We extracted all of the patients diagnosed with DPT in the participating institutions. A limitation of this retrospective study is that we could not determine the initial cohort, e.g. all of the subjects with asbestos exposure. The occupational categories in which the exposed patients had been employed, e.g. asbestos product manufacturing and shipbuilding, were associated with relatively high levels of asbestos. The median duration of asbestos exposure was 25 years, and the median period of latency from the first exposure to the onset of DPT was 47 years. Gibbs and Pooley [13] reported that, among the asbestos-related diseases, pulmonary asbestosis and lung cancer are associated with high levels of asbestos exposure, while malignant mesothelioma and DPT may develop after lower levels of exposure. Gibbs et al. [14] reported that >5 million asbestos fibers per gram of lung tissue were detected in 12 out of 13 patients with DPT. Our results provide support for these previous findings and suggest that DPT can develop after moderate-to-high levels of exposure to asbestos, because the occupational category of the subjects in the current study included those of relatively high levels of asbestos exposure, such as asbestos product manufacturing and shipbuilding. The median latency period between asbestos exposure and DPT development in the present study was similar to that observed for malignant mesothelioma and lung cancer in our previous reports [15–17] and that for DPT in another report by Kee et al. [18].

The prevalence of asbestos-related DPT is reported to range from 1.1 to 24.1% [3, 6, 19–21]. One of the reasons for this wide range could be variations in the diagnostic criteria for chest X-rays. Most patients, including ours, were originally diagnosed by chest X-ray based on dimension criteria; however, it is usually difficult to make a diagnosis or to evaluate DPT based solely on a chest X-ray. One of the purposes of the current study was to validate the utility of chest X-rays and CT to evaluate DPT. For this purpose, 2 independent researcher groups evaluated the presence or absence of pleural plaques, crow's feet signs, fibrotic changes, and emphysematous changes. Substantial κ were calculated for calcified pleural plaques, emphysematous changes, and crow's feet signs. More moderate coefficients were calculated for noncalcified plaques, fibrotic changes, and the involvement of the CPA, while the coefficients were low for the extension of DPT as determined by chest X-ray. These results indicate that the evaluation of DPT extension by chest X-ray is subjective and has a lower reliability, although the involvement of the CPA can be evaluated by chest X-ray.

Radiological differentiation between pleural plaques and DPT is often controversial [22]; however, this differentiation was not a critical issue in the current study because we focused on crow's feet and pleuroparenchymal fibrous strands [23] as indicators of the involvement of the visceral pleura and not of the plaques. In addition, a considerable number of patients in the current study had calcified plaques, possibly due to the long latency period since the initial asbestos exposure. These findings make it easier to differentiate pleural plaques from DPT.

The most common pattern of respiratory dysfunction in DPT is constrictive respiratory dysfunction [24, 25]. Therefore, in the current study, we investigated the main factors associated with %VC. We found that the mMRC dyspnea grade was the most important factor associated with an impaired %VC. DPT patients have been reported to complain of dyspnea on exertion relative to the amount of conserved respiratory function [4, 26]. When the visceral and parietal pleura conglutinate, the movement of the diaphragm may be impaired, particularly in cases in which the CPA is involved. This could lead to inhibition

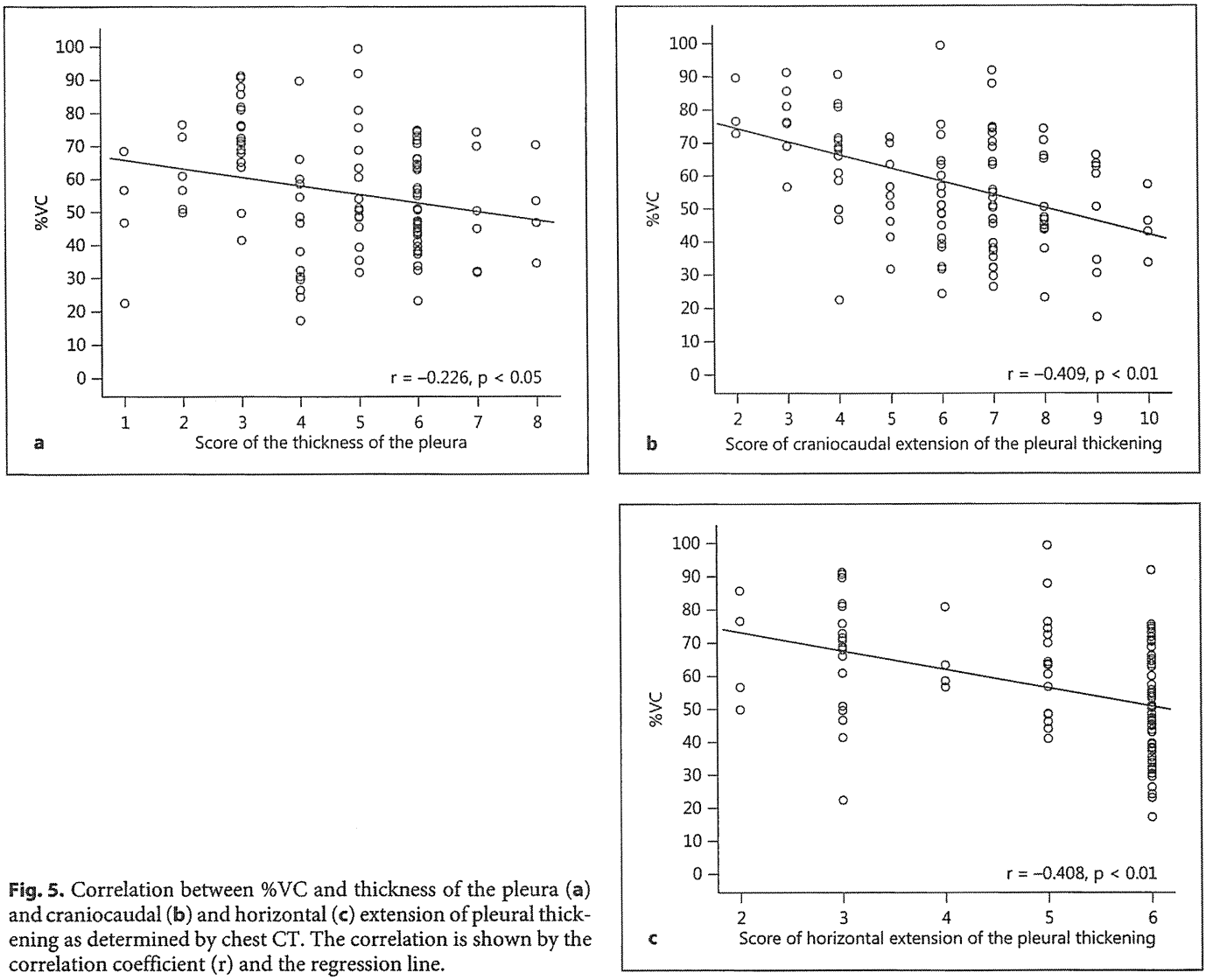

Fig. 5. Correlation between %VC and thickness of the pleura (**a**) and craniocaudal (**b**) and horizontal (**c**) extension of pleural thickening as determined by chest CT. The correlation is shown by the correlation coefficient (r) and the regression line.

of ventilation and to dyspnea on exertion. We evaluated the degree of dyspnea using the mMRC scale, but the mMRC scale is subjective; thus, more objective tools are necessary for the evaluation of DPT.

Among the radiological factors that we investigated, involvement of the CPA and craniocaudal and horizontal extension of pleural thickening were negatively correlated with %VC. Previous reports have described a correlation between involvement of the CPA and a reduced %VC [24, 27, 28]. In the current study, we demonstrated that the degree of involvement of the CPA was associated with a reduced %VC. In addition, bilateral involvement of the CPA tended to be associated with a reduced %VC. Craniocaudal and horizontal extension of pleural thickening was also associated with a reduced %VC, but this association was not strong. It is important that the extension of DPT was correlated with a reduced %VC when it was evaluated by chest X-ray and CT, but evaluation of the extension of DPT by chest X-ray is subjective, as described above. Therefore, we suggest that the extension of DPT should be evaluated by chest CT, which is a more accurate diagnostic method.

The pathogenic mechanisms of DPT are speculated to be as follows: (1) pulmonary asbestosis that spreads to the visceral and parietal pleura, (2) DPT that develops as a consequence of BAPE, and (3) DPT that develops independently of asbestosis or BAPE. In our study, 38 patients (35.5%) had some fibrotic changes, but asbestosis, defined as a profusion rate >1, was present in only 7 patients (6.6%). This rate is lower than that observed in a previous

report by McLoud et al. [6]. These results suggest that there is no obvious association between DPT and asbestosis. On the other hand, previous studies reported that a considerable number of patients with BAPE subsequently developed DPT [2, 3]. In the current study, half of the patients had a history of BAPE, and involvement of the CPA was shown in most of the cases with a history of BAPE. Thus, we believe that there is no direct association between asbestosis and DPT, but there is a strong link between BAPE and DPT.

The effect of smoking should be considered in conjunction with the respiratory embarrassment caused by inhalation of dust, such as asbestos [29, 30]. Finkelstein and Vingilis [31] reported that smokers had a 2.9-fold greater risk of DPT development compared to nonsmokers. In fact, the majority of patients in our study had smoked, and about 30% of the total cases demonstrated mixed ventilatory impairment. Cotes and King [24] reported that DPT patients demonstrated no significant changes in %FEV, but Kilburn and Warshaw [28] reported that some DPT cases had obstructive ventilatory impairment. The association between smoking and ventilatory impairment in DPT should be clarified in a future study.

In conclusion, we analyzed the clinical features of asbestos-related DPT and focused in particular on respiratory embarrassment. The mMRC dyspnea scale, the involvement of the CPA on chest X-ray, and the extension of pleural thickening on CT may be useful for evaluation of this disease.

Acknowledgements

This study is a part of the research and development and dissemination projects related to the 13 fields of occupational injuries and illnesses of the Japan Labour Health and Welfare Organization.

Financial Disclosure and Conflicts of Interest

All authors have no financial/nonfinancial disclosures.

References

1 American Thoracic Society: Diagnosis and initial management of nonmalignant diseases related to asbestos. Am J Respir Crit Care Med 2004;170:691–715.
2 Epler GR, McLoud TC, Gaensler EA: Prevalence and incidence of benign asbestos pleural effusion in a working population. JAMA 1982;247:617–622.
3 Hillerdal G: Non-malignant asbestos pleural disease. Thorax 1981;36:669–675.
4 Yates DH, Browne K, Stidolph PN, Neville E: Asbestos-related bilateral diffuse pleural thickening: natural history of radiographic and lung function abnormalities. Am J Respir Crit Care Med 1996;153:301–306.
5 Hillerdal G, Ozesmi M: Benign asbestos pleural effusion: 73 exudates in 60 patients. Eur J Respir Dis 1987;71:113–121.
6 McLoud TC, Woods BO, Carrington CB, Epler GR, Gaensler EA: Diffuse pleural thickening in an asbestos-exposed population: prevalence and causes. Am J Roentgenol 1985;144:9–18.
7 International Labour Office: Guidelines for the Use of the ILO International Classification of Radiographs of Pneumoconioses, rev ed. Geneva, International Labour Office, 2011, pp 6–8. http://www.ilo.org/safework/info/publications/WCMS_168260/lang–en/index.htm (accessed November 17, 2011).
8 Lilis R, Lerman Y, Selikoff IJ: Symptomatic benign pleural effusions among asbestos insulation workers: residual radiographic abnormalities. Br J Ind Med 1988;45:443–449.
9 de Klerk NH, Cookson WO, Musk AW, Armstrong BK, Glancy JJ: Natural history of pleural thickening after exposure to crocidolite. Br J Ind Med 1989;46:461–467.
10 Jeebun V, Stenton SC: The presentation and natural history of asbestos-induced diffuse pleural thickening. Occup Med 2012;62:266–268.
11 American Thoracic Society: Standardization of spirometry, 1994 update. Am J Respir Crit Care Med 1995;152:1107–1136.
12 Kundel HL, Polansky M: Measurement of observer agreement. Radiology 2003;228:303–308.
13 Gibbs AR, Pooley F: Mineral fiber analysis and asbestos-related diseases; in Craighead JE, Gibbs AR (eds): Asbestos and Its Diseases. New York, Oxford University Press, 2008, pp 296–316.
14 Gibbs AR, Stephens M, Griffiths DM, Blight BJ, Pooley FD: Fibre distribution in the lungs and pleura of subjects with asbestos related diffuse pleural fibrosis. Br J Ind Med 1991;48:762–770.
15 Kishimoto T, Gemba K, Fujimoto N, Aoe K, Kato K, Takeshima Y, Inai K: Clinical study on mesothelioma in Japan: relevance to occupational asbestos exposure. Am J Ind Med 2010;53:1081–1087.
16 Kishimoto T, Gemba K, Fujimoto N, Onishi K, Usami I, Mizuhashi K, Kimura K: Clinical study of asbestos-related lung cancer in Japan with special reference to occupational history. Cancer Sci 2010;101:1194–1198.
17 Gemba K, Fujimoto N, Kato K, Aoe K, Takeshima Y, Inai K, Kishimoto T: National survey of malignant mesothelioma and asbestos exposure in Japan. Cancer Sci 2012;103:483–490.
18 Kee ST, Gamsu G, Blanc P: Causes of pulmonary impairment in asbestos-exposed individuals with diffuse pleural thickening. Am J Respir Crit Care Med 1996;154:789–793.
19 Nemeth L, Tolnai K, Hovanyi E, Egervary M, Vincze E, Gyori S: Frequency, sensitivity and specificity of roentgenographic features of slight and moderate asbestos-related respiratory diseases. Rofo 1986;144:9–16.
20 Matrat M, Pairon JC, Paolillo AG, Joly N, Iwatsubo Y, Orlowski E, Letourneux, M, Ameille J: Asbestos exposure and radiological abnormalities among maintenance and custodian workers in buildings with friable asbestos-containing materials. Int Arch Occup Environ Health 2004;77:307–312.
21 Mastrangelo G, Ballarin MN, Bellini E, Bicciato F, Zannol F, Gioffre F, Zedde A, Tessadri G, Fedeli U, Valentini F, Scoizzato L, Marangi G, Lange JH: Asbestos exposure and benign asbestos diseases in 772 formerly exposed workers: dose-response relationships. Am J Ind Med 2009;52:596–602.

22 Fletcher DE, Edge JR: The early radiological changes in pulmonary and pleural asbestosis. Clin Radiol 1970;21:355–365.
23 Gevenois PA, de Maertelaer V, Madani A, Winant C, Sergent G, De Vuyst P: Asbestosis, pleural plaques and diffuse pleural thickening: three distinct benign responses to asbestos exposure. Eur Respir J 1998;11:1021–1027.
24 Cotes JE, King B: Relationship of lung function to radiographic reading (ILO) in patients with asbestos related lung disease. Thorax 1988;43:777–783.
25 Schwartz DA, Fuortes LJ, Galvin JR, Burmeister LF, Schmidt LE, Leistikow BN, LaMarte FP, Merchant JA: Asbestos-induced pleural fibrosis and impaired lung function. Am Rev Respir Dis 1990;141:321–326.
26 Miller A, Bhuptani A, Sloane MF, Brown LK, Teirstein AS: Cardiorespiratory responses to incremental exercise in patients with asbestos-related pleural thickening and normal or slightly abnormal lung function. Chest 1993; 103:1045–1050.
27 Bourbeau J, Ernst P, Chrome J, Armstrong B, Becklake MR: The relationship between respiratory impairment and asbestos-related pleural abnormality in an active work force. Am Rev Respir Dis 1990;142:837–842.
28 Kilburn KH, Warshaw RH: Abnormal lung function associated with asbestos disease of the pleura, the lung, and both: a comparative analysis. Thorax 1991;46:33–38.
29 Begin R, Filion R, Ostiguy G: Emphysema in silica- and asbestos-exposed workers seeking compensation: a CT scan study. Chest 1995; 108:647–655.
30 Hendrick DJ: Occupational and chronic obstructive pulmonary disease (COPD). Thorax 1996;51:947–955.
31 Finkelstein MM, Vingilis JJ: Radiographic abnormalities among asbestos-cement workers: an exposure-response study. Am Rev Respir Dis 1984;129:17–22.

Case Reports in Oncology

Case Rep Oncol 2014;7:389–392

DOI: 10.1159/000363760
Published online: June 14, 2014

1662–6575/14/0072–0389$39.50/0
www.karger.com/cro

Phrenic Nerve Paralysis as the Initial Presentation in Pleural Sarcomatoid Mesothelioma

Go Makimoto[a, c, d] Keiichi Fujiwara[a] Nobukazu Fujimoto[c]
Ichiro Yamadori[b] Toshio Sato[a] Takumi Kishimoto[c]

Departments of [a]Respiratory Medicine and [b]Laboratory Medicine, National Hospital Organization Okayama Medical Center, [c]Department of Respiratory Medicine, Okayama Rosai Hospital, and [d]Department of Allergy and Respiratory Medicine, Okayama University Hospital, Okayama, Japan

Key Words
Malignant pleural mesothelioma · Localized sarcomatoid mesothelioma · Phrenic nerve paralysis · Immunohistological examination

Abstract
A 74-year-old man was referred to our hospital because of persistent cough. A chest radiograph revealed an elevation of the right diaphragm. Computed tomography (CT) images revealed a small nodule localized on the right mediastinum. Five months later, the nodule had grown and was diagnosed as malignant pleural mesothelioma (MPM) by a CT-guided needle biopsy. The patient underwent combined chemotherapy, but the disease progressed rapidly and he passed away. On autopsy, microscopic findings and immunohistological examinations supported the diagnosis of sarcomatoid mesothelioma. Therefore, we diagnosed this rare case as localized sarcomatoid MPM showing phrenic nerve paralysis as an initial presentation.

Introduction

Malignant pleural mesothelioma (MPM) is a disease with poor prognosis. The median survival period is 7.7 months [1], and only an extrapleural pneumonectomy at an early stage can cure the disease. However, early detection of MPM is usually difficult, because its symptoms are nonspecific. In this study, we report a case of sarcomatoid MPM initially presenting as phrenic nerve paralysis.

Go Makimoto, MD
Department of Allergy and Respiratory Medicine
Okayama University Hospital
2-5-1 Shikata-cho, Kita-ku, Okayama 700-8558 (Japan)
E-Mail s_wolfjp@yahoo.co.jp

Case Report

A 74-year-old man was referred to our hospital because of persistent cough in October 2011. He had a history of prostate enlargement and gastric ulcer. He worked in the shipyard and had been exposed to asbestos for several years during his early twenties. He previously smoked 20 cigarettes per day for 24 years until he stopped smoking at the age of 44 years. A chest radiograph revealed an elevation of the right diaphragm (fig. 1a). Computed tomography (CT) images revealed a small nodule localized on the right mediastinum adjacent to the pericardial cavity (fig. 1b). Five months later, the nodule had developed into a massive tumor (fig. 1c). Finally, MPM was pathologically diagnosed by a CT-guided needle biopsy. The patient underwent combined chemotherapy with carboplatin and pemetrexed, but the disease progressed rapidly and caused superior vena cava syndrome. The patient then underwent palliative thoracic irradiation, but he passed away in June 2012. His family provided consent to conduct an autopsy.

On autopsy, a whitish solid tumor was detected on the right side of the mediastinum, and the tumor had infiltrated the parietal pleura, diaphragm, pericardial cavity, and aorta. The tumor had adhered strongly to the right upper lobe of the lung. Microscopically, the tumor consisted of spindle-shaped cells and collagen fibers, and had necrotic areas (fig. 2). Immunohistochemical examination revealed that the tumor cells were positive for calretinin, Wilms' tumor protein (WT-1), D2-40 and cytokeratin (AE1/AE3 and CAM 5.2), and negative for carcinoembryonic antigen (CEA) and thyroid transcription factor (TTF-1) (fig. 3). Diagnosis of sarcomatoid MPM was confirmed on the basis of these findings.

Discussion

MPM is classified into 2 types: diffused and localized. Localized MPM is uncommon and presents as a microscopic tumor characterized by a sharp circumscription of the serosal membrane without any evidence of diffused spread [2]. In the present case, a small localized tumor on the right chest wall was detected in October 2011. We suspected that the right phrenic nerve was involved with the tumor resulting in right phrenic nerve paralysis. At the beginning of the course, the lesion was localized. To our knowledge, this is the first report of MPM presenting phrenic nerve paralysis as an initial manifestation.

In order to confirm the diagnosis of sarcomatoid MPM, it is essential to distinguish it from lung sarcomatoid carcinoma (LSC). LSC is defined as an epithelial carcinoma consisting of spindle- or polygonal-shaped tumor cells, and is often a combination of the characteristics of adenocarcinoma or squamous cell carcinoma. It is difficult to differentiate sarcomatoid MPM from LSC; however, immunohistochemistry has proven to be useful in this regard [3]. Takeshima et al. [4] reported that the well-known mesothelial marker D2-40 was useful in differentiating sarcomatoid MPM from the sarcomatoid component of LSC. In our case, tumor cells were positive for both mesenchymal and epithelial markers, including D2-40, and negative for CEA and TTF-1. In addition, the radiological findings in the current case indicated that the primary lesion was apparently not in the lung. Therefore, a final diagnosis of MPM could be ascertained.

In conclusion, we report here a case of localized sarcomatoid MPM showing phrenic nerve paralysis as an initial presentation. It is important to perform immunohistochemical examination with sufficient materials to diagnose sarcomatoid MPM.

Disclosure Statement

The authors state that they have no conflict of interest.

References

1 Gemba K, Fujimoto N, Aoe K, et al: Treatment and survival analyses of malignant mesothelioma in Japan. Acta Oncol 2013;52:803–808.
2 Allen TC, Cagle PT, Churg AM, et al: Localized malignant mesothelioma. Am J Surg Pathol 2005;29:866–873.
3 Kushitani K, Takeshima Y, Amatya VJ, et al: Differential diagnosis of sarcomatoid mesothelioma from true sarcoma and sarcomatoid carcinoma using immunohistochemistry. Pathol Inter 2008;58:75–83.
4 Takeshima Y, Amatya VJ, Kushitani K, et al: Value of immunohistochemistry in the differential diagnosis of pleural sarcomatoid mesothelioma from lung sarcomatoid carcinoma. Histopathology 2009;54:667–676.

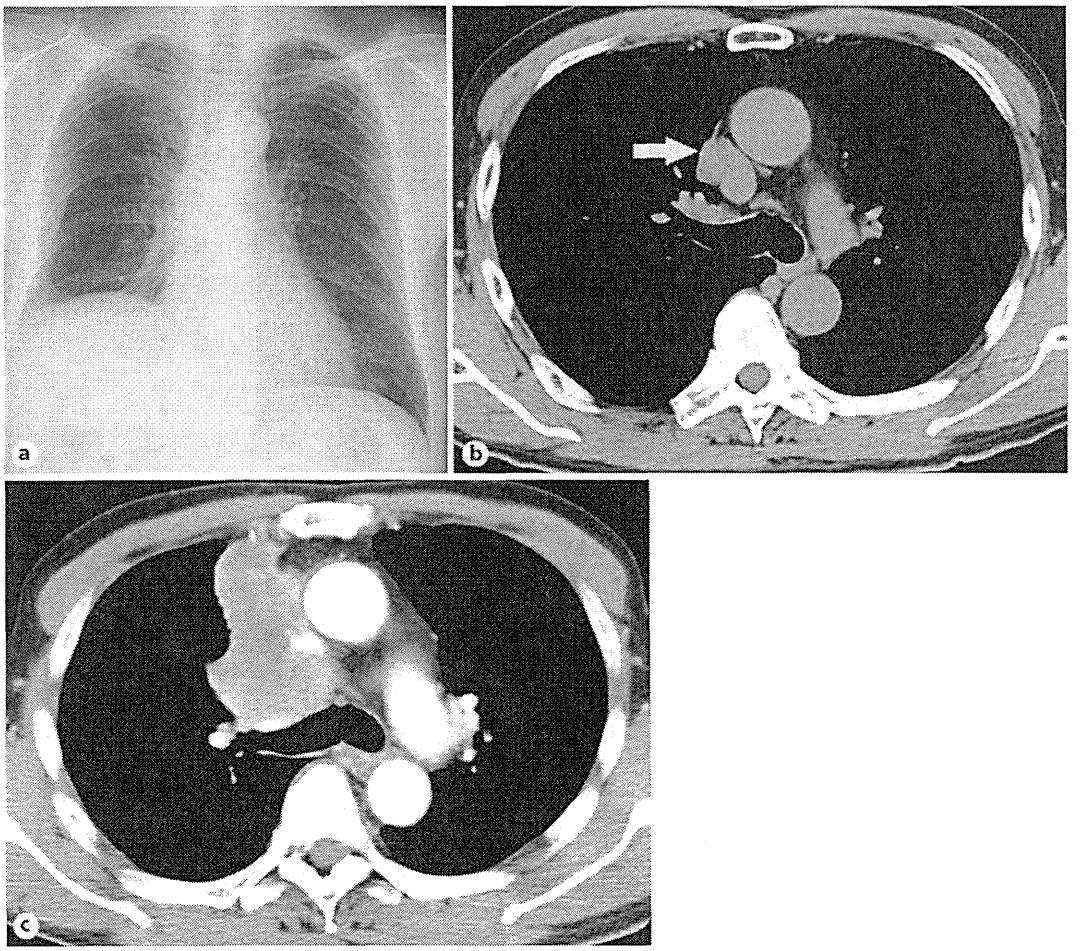

Fig. 1. A chest radiograph taken in October 2011 revealed elevation of the right diaphragm (**a**). CT images revealed a small nodule localized on the right mediastinum adjacent to the pericardial cavity (**b**). The nodule had developed into a massive tumor in March 2012 (**c**).

Case Rep Oncol 2014;7:389–392
DOI: 10.1159/000363760

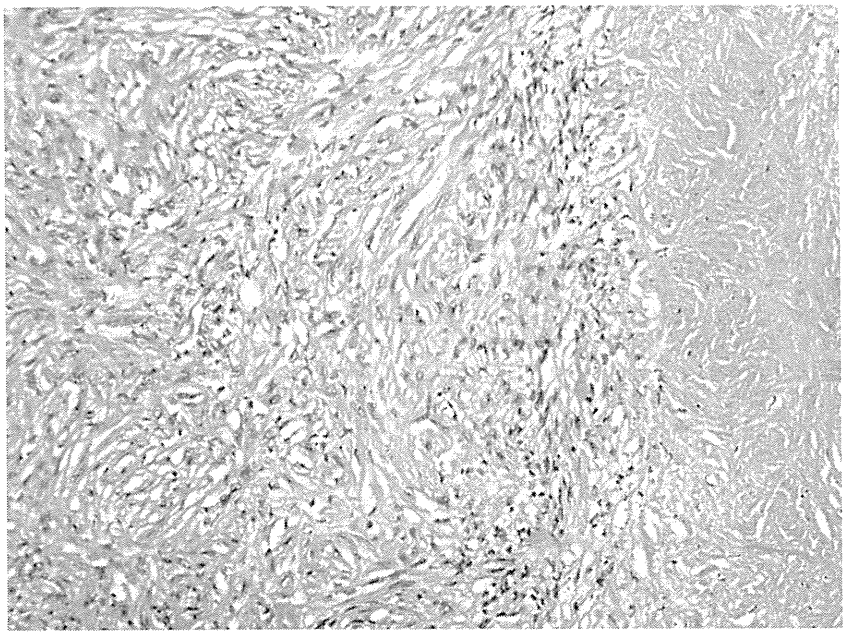

Fig. 2. During autopsy, histopathology of the mediastinal tumor revealed proliferation of spindle-shaped cells and collagen fibers with necrotic areas (hematoxylin and eosin stain).

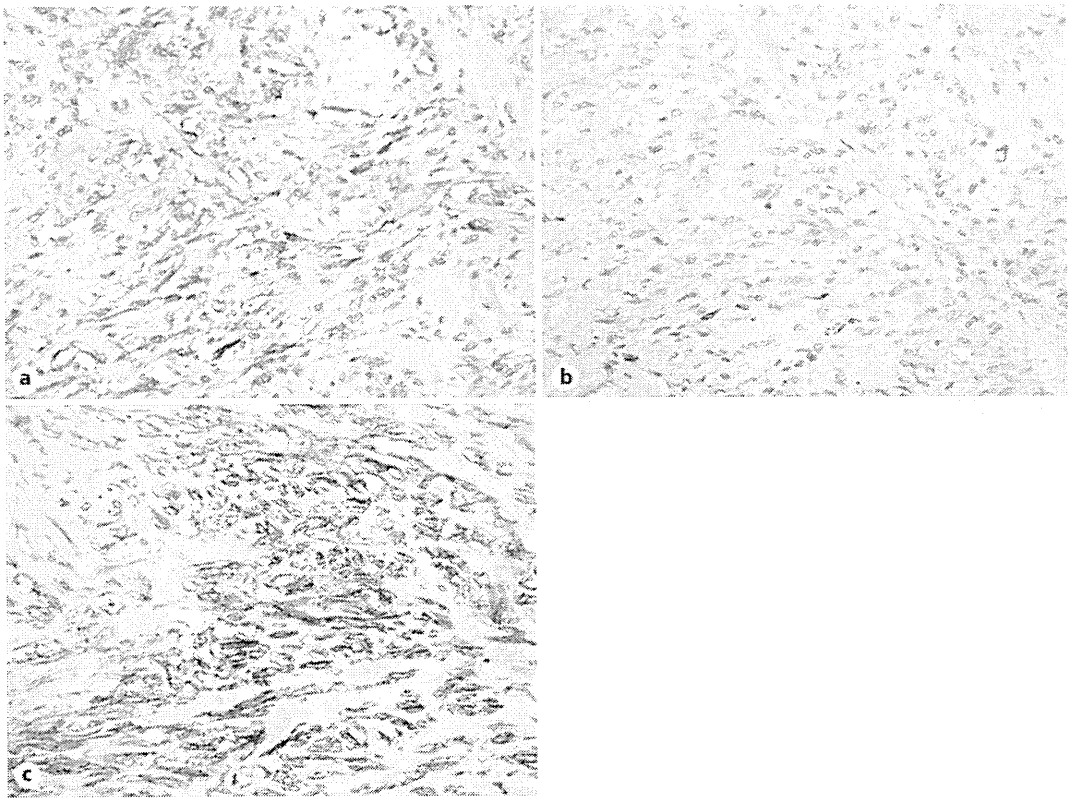

Fig. 3. Immunohistology revealed positive staining for calretinin (**a**), WT-1 (**b**), and D2-40 (**c**).

（肺癌．2014;54:767-771）

ORIGINAL ARTICLE

胸膜中皮腫を中心とした胸水ヒアルロン酸に関する症例調査

藤本伸一[1]・青江啓介[2]・大泉聡史[3]・上月稔幸[4]・
亀井敏昭[5]・三浦溥太郎[6]・井内康輝[7]・岸本卓巳[8]

Clinical Investigation of Hyaluronic Acid in Pleural Effusion

Nobukazu Fujimoto[1]; Keisuke Aoe[2]; Satoshi Oizumi[3]; Toshiyuki Kozuki[4];
Toshiaki Kamei[5]; Hirotaro Miura[6]; Kouki Inai[7]; Takumi Kishimoto[8]

[1]Department of Medical Oncology, Okayama Rosai Hospital, Japan; [2]Department of Medicine, National Hospital Organization Yamaguchi-Ube Medical Center, Japan; [3]Department of Respiratory Medicine, Hokkaido University Graduate School of Medicine, Japan; [4]Department of Medicine, National Hospital Organization Shikoku Cancer Center, Japan; [5]Department of Pathology, Yamaguchi Grand Medical Center, Japan; [6]Department of Medicine, Yokosuka General Hospital Uwamachi, Japan; [7]Pathological Diagnostic Center, Japan; [8]Department of Internal Medicine, Okayama Rosai Hospital, Japan.

ABSTRACT —— ***Objective.*** We evaluated the usefulness of assessing the hyaluronic acid (HA) level in pleural fluid for the differential diagnosis of malignant pleural mesothelioma (MPM). ***Methods.*** The data regarding the pleural fluid HA concentration were retrospectively collected from Rosai Hospitals and related facilities in Japan. ***Results.*** A total of 860 cases were examined, which included 139 cases of MPM, 76 of benign asbestos pleurisy (BAP), 324 of lung cancer (LC), 74 of other malignant conditions (OMC), 120 of infectious pleuritis (IP), 11 of collagen diseases (CD) and 116 cases had other conditions. The median (range) HA concentrations in the pleural fluid were 76,650 (211-33,000,000) ng/ml in the MPM cases, 28,000 (165-152,000) ng/ml in the BAP, 19,000 (800-134,000) ng/ml in the LC, 12,200 (900-157,200) ng/ml in the OMC, 23,400 (900-230,000) ng/ml in the IP, 17,800 (9,000-80,800) ng/ml in the CD and 11,575 (23-90,000) ng/ml in patients with other diseases. The HA levels were significantly higher in MPM cases than in the patients with other diseases. The receiver operating characteristics (ROC) analysis revealed an area under the ROC curve value of 0.818 (95% confidence interval, 0.772-0.864) for the differential diagnosis of MPM. With a cut-off value of 100,000 ng/ml, the sensitivity was 44.5% and the specificity was 98.2%. These results indicate that MPM should be strongly suspected in cases with an elevated concentration of pleural fluid HA. ***Conclusion.*** The pleural fluid HA concentrations might be useful for the differential diagnosis of MPM.

(*JJLC.* 2014;54:767-771)

KEY WORDS —— Asbestos, Hyaluronic acid, Mesothelioma, Pleural effusion, Tumor marker

Reprints: Nobukazu Fujimoto, Department of Medical Oncology, Okayama Rosai Hospital, 1-10-25 Chikkomidorimachi, Okayama 702-8055, Japan (e-mail: nobufujimot@gmail.com).

Received July 31, 2014; accepted September 5, 2014.

要旨 —— **目的．** 胸膜中皮腫の鑑別診断における胸水ヒアルロン酸の有用性を明らかにする．**方法．** 診療録より胸水ヒアルロン酸濃度を抽出し比較検討を行った．**結果．** 計860例分の胸水ヒアルロン酸濃度が抽出された．疾患の内訳は胸膜中皮腫139例，良性石綿胸水76例，肺癌324例，他臓器の悪性腫瘍74例，感染性胸膜炎120例，膠原病11例，その他116例であり，ヒアルロン酸濃度の中央値は胸膜中皮腫76,650 ng/ml，良性石綿胸水28,000 ng/ml，肺癌19,000 ng/ml，他臓器の悪性腫瘍12,200 ng/ml，感染性胸膜炎23,400 ng/ml，膠原病17,800 ng/ml，その他11,575 ng/mlであった．胸膜中皮腫における胸水ヒアルロン酸濃度はその他の疾患に比べ有意に高

[1]労働者健康福祉機構岡山労災病院腫瘍内科；[2]国立病院機構山口宇部医療センター内科；[3]北海道大学大学院医学研究科呼吸器内科学部門；[4]国立病院機構四国がんセンター内科；[5]山口県立総合医療センター病理科；[6]横須賀市立うわまち病院内科；[7]病理診断センター；[8]労働者健康福祉機構岡山労災病院内科．

別刷請求先：藤本伸一，労働者健康福祉機構岡山労災病院腫瘍内科，〒702-8055　岡山市南区築港緑町1-10-25（e-mail: nobufujimot@gmail.com）．

受付日：2014年7月31日，採択日：2014年9月5日．

値であり，カットオフ値を 100,000 ng/ml としたところ，胸膜中皮腫の診断における感度は 44.5%，特異度は 98.2% であった．**結論**．胸水中のヒアルロン酸濃度は，胸膜中皮腫の鑑別診断の一助となり得る．

索引用語 —— アスベスト，ヒアルロン酸，中皮腫，胸水，腫瘍マーカー

緒　言

胸膜中皮腫は胸膜の中皮細胞由来の予後不良な悪性腫瘍であり，[1] 石綿ばく露との関連が深い．[2,3] 胸膜中皮腫の確定診断は腫瘍組織からの生検組織を用いた病理診断に基づく．腫瘍組織を得るための最も有用な検査は胸腔鏡検査であり，中皮腫診断におけるゴールド・スタンダードといえる．胸腔鏡検査は，特に局所麻酔下にて施行される場合比較的侵襲は少ないものの，高齢者や合併症を有する患者の場合は本検査の適応から除外されるケースがしばしば見られる．このように，臨床的に胸膜中皮腫が疑われるものの確定診断が得られない，という症例は少なくない．

胸膜中皮腫においては診断時にその 70% 以上の症例で胸水貯留を呈する．[4] 胸水は臨床現場において比較的容易に採取することが可能であり，鑑別診断において重要な意味合いを持つが，胸水細胞診にて中皮腫の確定診断に達する症例は少なく，中皮腫のうち約 30% にとどまるといわれている．[5]

いわゆる分子生物学的マーカーは，各種の悪性腫瘍において高発現している分子の総称であり，その一部はある種の悪性腫瘍の補助診断や治療効果のモニタリングに臨床応用されている．胸膜中皮腫においてもこれまでにいくつかの分子マーカーが着目され，診断のための有用性について検討されている．なかでもヒアルロン酸は，以前より胸膜中皮腫の胸水中に高濃度で存在することが知られており，[6-8] 細胞外マトリクスの主成分として中皮腫細胞の移動や発育に重要な役割を果たしている．Pettersson らの報告では，カットオフ値を 100,000 ng/ml とした場合，胸膜中皮腫では 73% が陽性，炎症性胸膜炎で 23% が陽性であったが，その他の悪性腫瘍や心不全では 1 例も陽性例は認められなかったと報告している．[6] 悪性中皮腫以外でも，ウイルス性胸膜炎や関節リウマチ患者の胸水中のヒアルロン酸濃度が高値を呈するとの報告がある．[7] この他，頻度は低いものの癌性胸膜炎，良性石綿胸水，心不全でも同様の報告がある．[8] われわれはこれまでに，単一施設における後ろ向きの検討を行い他疾患との鑑別，および胸膜中皮腫の診断における胸水ヒアルロン酸の有用性について検討した．[9] 本研究では，多施設より胸膜中皮腫症例や他の胸水貯留症例を収集し，胸水ヒアルロン酸濃度を胸膜中皮腫診断の指標として用いる意義について検証した．

研究対象，方法

2001 年 8 月から 2010 年 10 月までの間に，全国各労災病院および本研究における研究協力施設において，胸水貯留をきたし，診断目的にて胸水採取を行われた症例を後ろ向きに集積し，診療録より胸水中のヒアルロン酸濃度を抽出した．ヒアルロン酸濃度は各施設より委託された外部検査施設においてラテックス凝集法にて測定されていた．これらの症例を胸膜中皮腫，良性石綿胸水，肺癌，胸膜中皮腫と肺癌以外の悪性腫瘍，感染性胸膜炎，膠原病，その他の疾患に分類し比較検討した．また可能な限り carcinoembryonic antigen(CEA)，アデノシンデアミナーゼ(ADA)値についてもデータを収集した．データの収集に当たっては，厚生労働省の「疫学研究に関する倫理指針」を遵守し，労働者健康福祉機構が定める倫理審査手順に沿って同機構が妥当性の評価を行った．統計学的手法としては，多群間の比較には Kruskal-Wallis 検定を用い，独立した 2 群間の比較には Mann-Whitney 検定を用いた．

結　果

上記の期間中に胸水中のヒアルロン酸濃度が測定され，本研究のために集積された症例は 860 例であった．各施設における疾患別の症例集積数を Table 1 に示す．疾患群毎の内訳は，胸膜中皮腫 139 例，良性石綿胸水 76 例，肺癌 324 例，他臓器の悪性腫瘍の胸腔内転移 74 例，感染性胸膜炎 120 例，膠原病 11 例，その他の疾患 116 例である．その他の疾患の大半はうっ血性心不全，肝硬変が占めた．

胸水中のヒアルロン酸濃度の中央値（範囲）は，胸膜中皮腫 76,650 ng/ml (211～33,000,000 ng/ml)，良性石綿胸水 28,000 ng/ml(165～152,000 ng/ml)，肺癌 19,000 ng/ml (800～134,000 ng/ml)，他臓器の悪性腫瘍の胸腔内転移 12,200 ng/ml (900～157,200 ng/ml)，感染性胸膜炎 23,400 ng/ml(900～230,000 ng/ml)，膠原病 17,800 ng/ml (9,000～80,800 ng/ml)，その他の疾患では 11,575 ng/ml (23～90,000 ng/ml) であった (Figure 1)．胸膜中皮腫とそれ以外の疾患において Kruskal-Wallis 検定を用いて比較したところ，明らかな有意差が認められた($P<0.001$)．Mann-Whitney 検定を用いた 2 群間の比較では，胸膜中

Table 1. The Numbers of Cases Collected at Each Facility

	n	Disease						
		MPM*	BAPE†	LC‡	OMC§	IP‖	CD¶	Others
Okayama Rosai Hospital	336	51	45	81	22	69	6	62
Yamaguchi-Ube Medical Center	183	27	15	88	10	23	5	15
Shikoku Cancer Center	160	12	3	92	32	5	0	16
Kagawa Rosai Hospital	109	5	9	42	9	23	0	21
Hokkaido University Hospital	32	10	0	20	1	0	0	1
Kanto Rosai Hospital	6	6	0	0	0	0	0	0
Tokyo Rosai Hospital	6	5	1	0	0	0	0	0
Chiba Rosai Hospital	5	5	0	0	0	0	0	0
Asahi Rosai Hospital	5	3	2	0	0	0	0	0
Tohoku Rosai Hospital	4	4	0	0	0	0	0	0
Hokkaido Chuo Rosai Hospital	3	3	0	0	0	0	0	0
Toyama Rosai Hospital	3	3	0	0	0	0	0	0
Yamaguchi Rosai Hospital	3	3	0	0	0	0	0	0
Nagasaki Rosai Hospital	3	2	1	0	0	0	0	0
Kashima Rosai Hospital	1	0	0	0	0	0	0	1
Hamamatsu Rosai Hospital	1	0	0	1	0	0	0	0
Total	860	139	76	324	74	120	11	116

*malignant pleural mesothelioma, †benign asbestos pleural effusion, ‡lung cancer, §other malignant condition, ‖infectious pleuritis, ¶collagen disease.

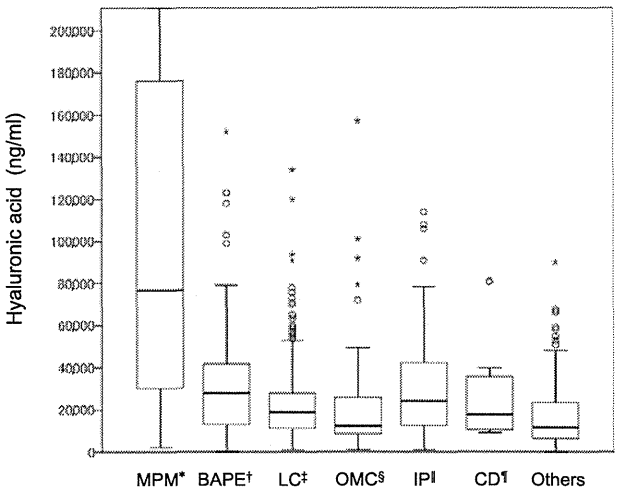

Figure 1. Comparison of the hyaluronic acid concentrations in pleural fluid. *malignant pleural mesothelioma, †benign asbestos pleural effusion, ‡lung cancer, §other malignant condition, ‖infectious pleuritis, ¶collagen disease.

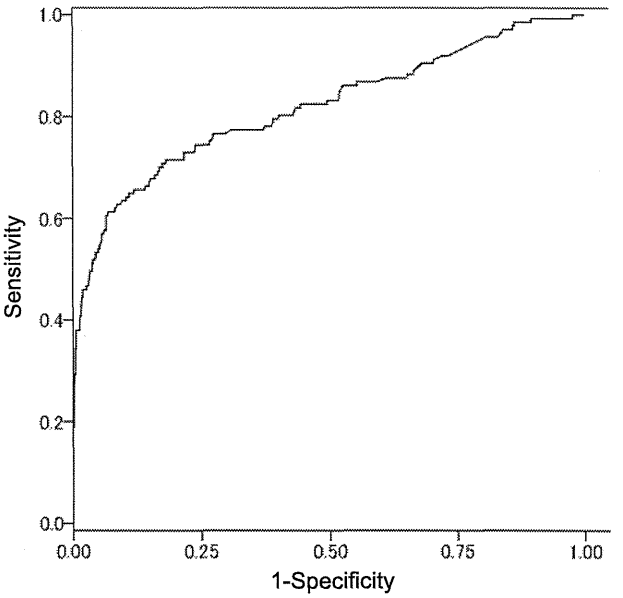

Figure 2. The results of the receiver operating characteristics analysis of the use of the hyaluronic acid concentration for the differential diagnosis of malignant pleural mesothelioma.

皮腫と他の疾患群の間には明らかな有意差が認められた．次に胸膜中皮腫とそれ以外の症例について，receiver operating characteristics（ROC）曲線を作成し検討したところ，area under the ROC curve（AUC）値は 0.818（95% 信頼区間 0.772～0.864）であった（Figure 2）．Youden's index[10] を用いて得られた最適のカットオフ値は 59,650 ng/ml であり，その際の胸膜中皮腫の診断における感度は 61.3%，特異度は 93.1% であった．またカットオフ値を 100,000 ng/ml, 150,000 ng/ml, 200,000 ng/ml とした場合の感度はそれぞれ 44.5%，29.2%，22.6% であり，特異度はそれぞれ 98.2%，99.6%，99.9% であった．

胸水中のヒアルロン酸濃度が 100,000 ng/ml 以上で

Table 2. The Features of the Cases Other Than Malignant Pleural Mesothelioma with a Hyaluronic Acid Concentration More Than 100,000 ng/ml

Case	Disease	Hyaluronic acid (ng/ml)	CEA[§] (ng/ml)	ADA[¶] (IU/l)
1	Pharyngeal cancer	101,000	83.1	15.6
2	BAPE*	103,000	0.9	30.2
3	Pleuritis	106,000	2.2	16.9
4	Tbc[†]	108,000	3.2	123.4
5	Tbc	114,000	1.8	114.5
6	BAPE	118,000	1.5	13.6
7	LC[‡]	120,000	2.1	16.1
8	BAPE	123,000	3.1	17.7
9	BAPE	123,000	0.9	18.7
10	LC	134,000	13979.4	149.0
11	BAPE	152,000	0.9	21.5
12	Renal cancer	157,200	ND[‖]	32.3
13	Pyothorax	230,000	4.8	ND

*benign asbestos pleural effusion, [†]tuberculous pleuritis, [‡]lung cancer, [§]carcinoembryonic antigen, [‖]not determined, [¶]adenosine deaminase.

あった症例は860例中74例で，全体の8.6%であった．これらの74例のうち61例（82.4%）は胸膜中皮腫であり，胸膜中皮腫以外で100,000 ng/ml以上であった例はTable 2に示す13例（全体の1.5%）であり，内訳は良性石綿胸水が5例，結核性胸膜炎が2例，肺癌が2例，咽頭癌，腎癌の胸腔内転移がそれぞれ1例ずつ，結核以外の感染性胸膜炎が2例（膿胸の1例を含む）であった．このうち，結核性胸膜炎の2例は，Table 2に示すように胸水中のADA値がそれぞれ123.4 IU/l，114.5 IU/lと著明な高値を呈しており，またいずれの症例においても発熱などの感染症状に加え，PCR法による胸水中の遺伝子検索にて結核菌の存在が証明されていた．また肺癌の2例は胸水細胞診において疑義の余地なく肺癌と診断されていた．このうち1例はTable 2に示すように胸水中のCEA値が著明な高値を呈していた．腎癌の症例についても臨床経過より診断には疑義の余地はなかった．感染性胸膜炎と診断されている2例は，いずれも発熱などの感染症状や炎症反応などを呈し，特に膿胸の症例は特異的な胸水の性状などから臨床診断に疑義の余地は見られなかった．それ以外の咽頭癌の1例と良性石綿胸水の5例については臨床経過や画像を含めた検査所見からの診断は困難であり，診断の確定には胸腔鏡下胸膜生検を要した．

考　察

われわれは最近，岡山労災病院における胸膜中皮腫並びに他の疾患における胸水中のヒアルロン酸濃度を中心に解析した．その結果，1)胸水中のヒアルロン酸濃度が100,000 ng/mlを上回る場合，その大半の症例は胸膜中皮腫であること，2)中皮腫以外の疾患である場合，他の臨床徴候，画像所見，あるいは胸水の性状や抗酸菌を含む細菌学的な検討を加えることで，肺癌や結核性胸膜炎を含めた感染性胸膜炎の大半は臨床診断が可能であること，3)良性石綿胸水において胸水中のヒアルロン酸濃度が100,000 ng/mlを上回る症例が散見されること，を報告した.[9] ただその際の検討では特に胸膜中皮腫以外の疾患の症例集積数は十分とはいえず，多施設，多症例における検討が必要と思われた．本研究では前述の岡山労災病院のデータに加え全国の各労災病院，および北海道大学病院，国立病院機構四国がんセンター，国立病院機構山口宇部医療センターを中心にデータを加え，860例に及ぶデータが集積された．各施設の特徴を反映して疾患の分布に多少の違いがあるものの，ある程度実臨床を反映した疾患の分布といえると思われる．その結果今回の検討でも，胸膜中皮腫では他の胸水を呈する疾患に比べ明らかにヒアルロン酸濃度は高値を呈しており，胸膜中皮腫の診断マーカーとしての有用性が改めて示唆された．実臨床において胸膜中皮腫を強く疑う目安の数値とされている100,000 ng/mlをカットオフ値とした場合，胸膜中皮腫の診断における感度は44.5%，特異度は98.2%に達していた．このことから，胸水ヒアルロン酸濃度が高値である場合，まず胸膜中皮腫を念頭に置く必要があることが改めて示されたと考える．

胸膜中皮腫の確定診断は病理診断によるものであり，胸腔鏡などの検査により十分量の腫瘍組織を元に各種の免疫組織学的検索を踏まえた上で診断されるべきであるが，胸膜中皮腫患者の多くは過去の石綿ばく露から30年から40年に及ぶ潜伏期間を経て発症することが多い

ため，高齢であることが多く，合併症などのため侵襲を伴う検査が見送られるケースが少なからずある．今回の検討において，胸水ヒアルロン酸濃度が100,000 ng/ml以上であった場合，胸膜中皮腫である確率は74例のうち61例で82.4%である．このカットオフ値で，ヒアルロン酸値のみで中皮腫と診断した場合，13例が偽陽性，つまり中皮腫でないのに中皮腫と診断されることとなる．しかしTable 2に示したこれらの症例のうち，約半数は発熱などの臨床徴候や検査所見，画像所見より臨床診断が比較的容易になされている．ただこれらの症例を除く下咽頭癌の1例と良性石綿胸水の5例については，臨床経過や画像を含めた検査所見からの診断は困難であり，診断の確定には胸腔鏡下胸膜生検を要した．なおこれらの良性石綿胸水の5例は，その後の経過観察においても胸膜中皮腫の発症は認められていない．この結果より，胸水中のヒアルロン酸濃度に一般臨床において通常施行されうる検査所見を加えることにより，大半の症例は臨床診断に到達しうるといえる．具体的には，発熱などの感染症状の有無，血液検査における白血球数，CRP値などの炎症所見の有無，画像所見，さらには胸水の性状，細胞診に加え一般細菌や抗酸菌の塗抹，培養，および結核菌群核酸同定（PCR法）などがあげられる．さらに他の胸水マーカーとしてCEA，ADAなどもその一助となり得る．たとえばTable 2に示した咽頭癌の1例と肺癌の2例のうちの1例では胸水CEA値が著明な高値を呈しており，胸膜中皮腫以外の疾患を示唆する所見といえる．またADAは結核性胸膜炎において高値を呈することが多く，一般的に40 IU/*l*を上回る場合は結核性胸膜炎である可能性が高いといわれているが，[11,12] 今回の検討ではそれ以外の疾患群においても40 IU/*l*を上回る症例も散見されており，鑑別診断には慎重である必要がある．

これまで述べてきたように，胸水中のヒアルロン酸濃度は胸膜中皮腫の鑑別診断において有用である．実臨床における有用性のみならず，石綿健康被害救済制度などの運用において，高齢や合併症など何らかの理由により病理診断が得られていないものの胸水中のヒアルロン酸濃度が高値を呈する症例において，1)胸膜の腫瘍性肥厚，不整な肥厚など画像的に胸膜中皮腫として矛盾しないこと，2)発熱や炎症反応など，明らかに感染症を疑わせる所見がないこと，3)CEAやADAが極端な高値でないことなどを確認し，さらに臨床経過などを十分吟味し胸膜中皮腫を認定していくことも考慮すべきと思われる．ただ本来は胸膜中皮腫の診断は病理診断によるものであり，胸腔鏡などの検査により十分量の腫瘍組織を元に各種の免疫組織学的検索を踏まえた上で診断されるべきである．

本論文内容に関連する著者の利益相反：なし

謝辞：本研究は，環境省請負業務「平成23年度石綿関連疾患に係る医学的所見の解析調査（胸水ヒアルロン酸，胸水腫瘍マーカー測定値に基づく中皮腫診断補助検査の確立に関する調査編）」の一部として行った．また本研究は独立行政法人労働者健康福祉機構「労災疾病等13分野医学研究・開発・普及事業」によるものである．

REFERENCES

1. Gemba K, Fujimoto N, Aoe K, Kato K, Takeshima Y, Inai K, et al. Treatment and survival analyses of malignant mesothelioma in Japan. *Acta Oncol.* 2013;52:803-808.
2. Gemba K, Fujimoto N, Kato K, Aoe K, Takeshima Y, Inai K, et al. National survey of malignant mesothelioma and asbestos exposure in Japan. *Cancer Sci.* 2012;103:483-490.
3. Kishimoto T, Gemba K, Fujimoto N, Aoe K, Kato K, Takeshima Y, et al. Clinical study on mesothelioma in Japan: Relevance to occupational asbestos exposure. *Am J Ind Med.* 2010;53:1081-1087.
4. Fujimoto N, Aoe K, Gemba K, Kato K, Yamazaki K, Kishimoto T. Clinical investigation of malignant mesothelioma in Japan. *J Cancer Res Clin Oncol.* 2010;136:1755-1759.
5. Renshaw AA, Dean BR, Antman KH, Sugarbaker DJ, Cibas ES. The role of cytologic evaluation of pleural fluid in the diagnosis of malignant mesothelioma. *Chest.* 1997;111:106-109.
6. Pettersson T, Fröseth B, Riska H, Klockars M. Concentration of hyaluronic acid in pleural fluid as a diagnostic aid for malignant mesothelioma. *Chest.* 1988;94:1037-1039.
7. Hillerdal G, Lindqvist U, Engström-Laurent A. Hyaluronan in pleural effusions and in serum. *Cancer.* 1991;67:2410-2414.
8. Söderblom T, Pettersson T, Nyberg P, Teppo AM, Linko L, Riska H. High pleural fluid hyaluronan concentrations in rheumatoid arthritis. *Eur Respir J.* 1999;13:519-522.
9. Fujimoto N, Gemba K, Asano M, Fuchimoto Y, Wada S, Ono K, et al. Hyaluronic acid in the pleural fluid of patients with malignant pleural mesothelioma. *Respir Investig.* 2013;51:92-97.
10. Youden WJ. Index for rating diagnostic tests. *Cancer.* 1950;3:32-35.
11. 青江啓介，平木章夫，村上知之．結核性胸膜炎の診断と治療—とくに胸水中サイトカイン測定の意義について—．結核．2004;79:289-295.
12. Ogata Y, Aoe K, Hiraki A, Murakami K, Kishino D, Chikamori K, et al. Is adenosine deaminase in pleural fluid a useful marker for differentiating tuberculosis from lung cancer or mesothelioma in Japan, a country with intermediate incidence of tuberculosis? *Acta Med Okayama.* 2011;65:259-263.